PETROGRAPHY AND GEOCHEMISTRY OF THE EARLY-MIDDLE DEVONIAN SANDSTONES OF THE PADEHA FORMATION IN THE NORTH OF KERMAN, SE IRAN. IMPLICATIONS FOR PROVENANCE

Hamed ZAND-MOGHADAM, Reza MOUSSAVI-HARAMI, Asadollah MAHBOUBI & Behnam RAHIMI

Boletín
del Instituto de
Fisiografía y Geología

Abstract.- This study presents a petrological and geochemical characterization of the Early-Middle Devonian sandstones of the Padeha Formation in SE Central Iran, north of Kerman in order to determine the provenance on the basis of two measured stratigraphic sections. The sandstones are classified as quartzarenite and sublitharenite, and subordinately as litharenite based on framework composition. Modal analysis data from 55 samples of the Sarashk and Gazuieh sections revealed that the sandstones contain quartz, a few percent feldspars and lithic fragments (sedimentary and volcanic rocks). Most of the quartz grains are monocrystalline with straight to undulate extinction with a few polycrystalline grains. Petrographic studies indicate that the Padeha Formation sandstones may have been derived from plutonic and other recycled orogen rocks. Chemically, the major oxides of the sandstones from the Sarashk section are depleted with respect to the upper continental crust, except SiO_2, which is related to the high maturity (presence of quartz) and the absence of Al-bearing minerals (phyllosilicates). The trace element concentrations (La, Th, Sc and Zr) and La/Sc (5.50-16.57), Th/Sc (1.12-4.14), La/Co (1.97-20.66), and Th/Co (0.72-4.75) of the Sarashk section indicate felsic source rocks for the sandstones. Furthermore, high Zr/Sc (48-368) and Th/U (0.5-6.8) values are typical for recycling. The chondrite-normalized rare earth element (REE) patterns support this interpretation. Light REE enrichment, negative Eu anomaly and flat heavy REE pattern are very similar to the old upper continental crust. Combined petrological-geochemical data and local Devonian palaeogeographical models show that the Padeha Formation sandstones mostly derived from felsic source rocks and mature recycled continental sedimentary rocks in the craton interior of Central Iran and adjacent areas and were deposited on the passive margin along the coastal setting of the Paleo-Tethys Ocean.

Key Words: Petrography, Geochemistry, Provenance, Sandstone, Padeha Formation, Kerman, Iran.

Resumen.- *Petrografía y geoquímica de las areniscas del Devónico Temprano a Medio de la Formación Padeha en el Norte de Kerman, SE Iran. Implicancias acerca de la proveniencia.* Este informe presenta los resultados de un estudio de caracterización petrológica y geoquímica de las areniscas de la Formación Padeha en el Norte de Kerman (SE de Irán). El objetivo principal de este estudio es determinar la proveniencia sobre la base de dos secciones estratigráficas medidas a tal efecto. Las areniscas son clasificadas según su composición como arenitas cuarcíticas y sublitarenitas, y subordinadamente litarenita. Los datos de un análisis modal realizado sobre 55 muestras de las secciones estudiadas, Sarashk y Gazuieh, indica que las areniscas contienen cuarzo, escaso feldespato y fragmentos líticos (rocas sedimentarias y volcánicas). La mayoría de los granos de cuarzo son monocristalinos con extinción recta u ondulada, con escasos granos policristalinos. El estudio petrográfico indica que las areniscas de la Formación Padeha fueron derivadas de rocas plutónicas y otras de orógeno reciclado. Químicamente la presencia de la mayor parte de los óxidos de las areniscas de la sección de Sarashk está reducida, excepto SiO2, lo cual está relacionado con la alta madurez (presencia de cuarzo) y la ausencia de minerales con contenido de Al (filosilicatos). Las concentraciones de elementos traza de la sección de Sarashk (La, Th, Sc and Zr) y las proporciones La/Sc (5.50-16.57), Th/Sc (1.12-4.14), La/Co (1.97-20.66) y Th/Co (0.72-0.75) indican una fuente de rocas félsicas. Por otra parte se han detectado valores altos de Zr/Sc (48-368) y Th/U (0.5-6.8) lo cual es típico de un proceso de reciclado. Los patrones de presencia de tierras raras normalizadas respecto a condrita apoyan esta interpretación. El enriquecimiento en tierras raras livianas, la anomalía negativa de Eu y un patrón plano de tierras raras pesadas son muy similares a las que caracterizan a la antigua corteza continental superior. La consideración de datos petrológicos y geoquímicos junto a los modelos de paleogeografía Devónica local muestran que las areniscas de la Formación Padeha fueron derivadas mayormente de rocas félsicas y rocas sedimentarias del cratón inferior de Irán central y áreas adyacentes, y depositadas en el márgen pasivo a lo largo de un dispositivo de costa marina del Océano Paleotethys.

Palabras clave: Petrografía, Geoquímica, Proveniencia, Areniscas, Formación Padeha, Kerman, Irán.

Adress of the authors:

Hamed Zand-Moghadam [Zand1883@yahoo.com]
Reza Moussavi-Harami
Asadollah Mahboubi
Behnam Rahimi.
Department of Geology, Faculty of Science, Ferdowsi University of Mashhad,
Iran
Fax and Tel: +98 511 8797275

Bol. Inst. Fis. Geol. **83 (2013)**: 1-14
Rosario - Argentina.

Copia Impresa / Printed Copy [€ 14+5]
http://www.fceia.unr.edu.ar/fisiografia

INTRODUCTION

During the Silurian and Devonian, parts of Iran (Central Iran, Alborz, and Sanandaj-Sirjan) along with the Afghan and Turkish plates were attached to the Arabian and African plates and formed the northwestern margin of Gondwana and the southern margin of the Paleo-Tethys (Berberian & King 1981, Husseini 1991, Sharland et al. 2001, Ruban et al. 2007, Al-Juboury & Al-Hadidy 2009). The positions of these plates were determined mostly by geometric data, but a precise position of fragments of Central Iran and Alborz is not well defined. However, many authors such as Gaeley (1977), Sengör et al. (1988), and Husseini (1991) demonstrated the united terrane consisting of the Central Iran and Afghan terranes in a close proximity, whereas Ruban et al. (2007) suggested that the two terranes were separated. The sea level dropped sharply at the beginning of Devonian time (Vail et al. 1977) when siliciclastic rocks of the Padeha Formation and equivalent rocks formed in most parts of northern Gondwana. Generally, the Lower-Middle Devonian succession is absent in most parts of the Middle East due to erosion during the Hercynian orogeny (Husseini 1991). The rock units are the Tawil and Jauf formations in Saudi Arabia, Kuwait (partly), United Arab Emirates, and Qatar; the Dadas, Hazro, Sigircik, Zeitoun and Aytepesi formations in Turkey; the Padeha Formation in central Iran and parts of Muli and Zakeen formations in NW and South of Iran respectively (Husseini 1991, Ghavidel-Syooki 1994, Al-Sharhan & Narin 1997, Al-Hajri & Filatoff 1999, Brew & Barazangi 2001, Sharland et al. 2001, Wendt et al. 2002, 2005, Laboun 2010, Wehrmann et al. 2010; see Fig. 1). These formations were mostly deposited in fluvial-coastal (Saudi Arabia) to coastal-shallow marine settings (Iran and Turkey). The precise depositional timing for the Early-Middle Devonian sedimentary rocks is unclear due to the lack of time-diagnostic fossils.

Few previous studies focused on the sedimentological aspects of the Padeha Formation (e.g. Aharipour et al., 2010, Zand-Moghadam et al. 2013a,b), especially in the Tabas Block.

The most comprehensive study on the Devonian rocks in Iran was carried out by Wendt et al. (2002, 2005). They believed that the Early-Middle Devonian rocks (the Padeha Formation) were deposited mainly in a siliciclastic shelf at the northern margin of Gondwana that is delineated by land areas in the north (central and eastern Alborz), southeast (Lut Block), and southwest (Zagros). In this study, we used the petrographical and geochemical methods to interpret the provenance and tectonic setting of the Padeha Formation sandstones in the Sarashk (30°50'58" N, 57°01'57.8" E) and Gazuieh (30°50'54.31" N, 56°41'48.35" E) sections north of Kerman, SE Iran (Fig. 2). The type section of the Padeha Formation located at the Ozbak-Kuh mounntains (Tabas area) is composed of siliciclastic sedimentary rocks, dolomite and evaporites deposited in tidal flat and sabkha environments (Zand-Moghadam et al. 2013a). On the other hand, the Padeha Formation north of Kerman is mostly composed of siliciclastic sedimentary rocks (Fig. 3; Huckriede et al. 1962, Vahdati-Daneshmand et al. 1995, Zand-Moghadam et al. 2013b).

The main purpose of this study is to interpret the source rocks and tectonic setting of the Padeha Formation sandstones. Then, we briefly discuss the palaeogeographic implications of the results obtained for the interval Early-Middle Devonian on local and regional scales.

GEOLOGICAL SETTING

The study area is located in the central part of the Central-East Iranian Microcontinent (CEIM; Takin 1972, Stocklin 1974; Fig. 2). The CEIM, together with central Iran and the Alborz Mountains, forms the Iran Plate, which occupies a structural key position in the Middle Eastern Tethysides (Sengör et al. 1988, Sengör 1990). The CEIM consists of three north-south oriented structural units, called the Lut, Tabas, and Yazd Blocks (Fig. 2A-B), which are now aligned from east to west, respectively (Stocklin 1968, 1977).

The rock succession exposed in this area includes all
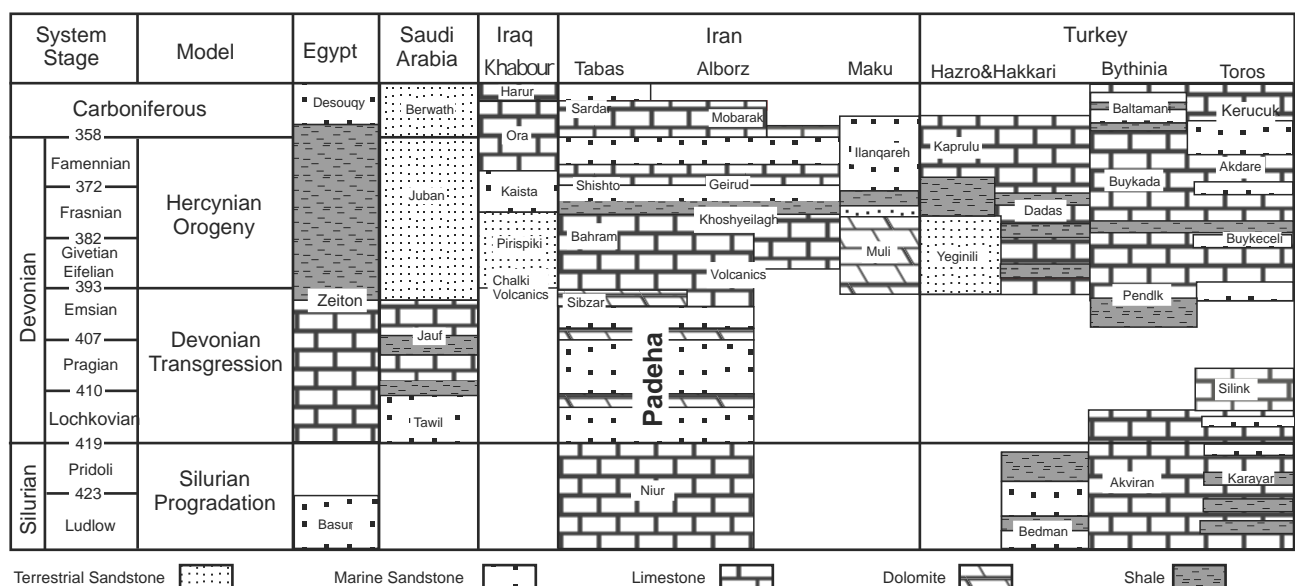
Figure 1. Time-correlation chart of the Devonian rock lithostratigraphic units (formations) of Iran, Saudi Arabia, Egypt, Turkey and Iraq (modified from Husseini 1991). Numerical ages from Gradstein et al. (2012).
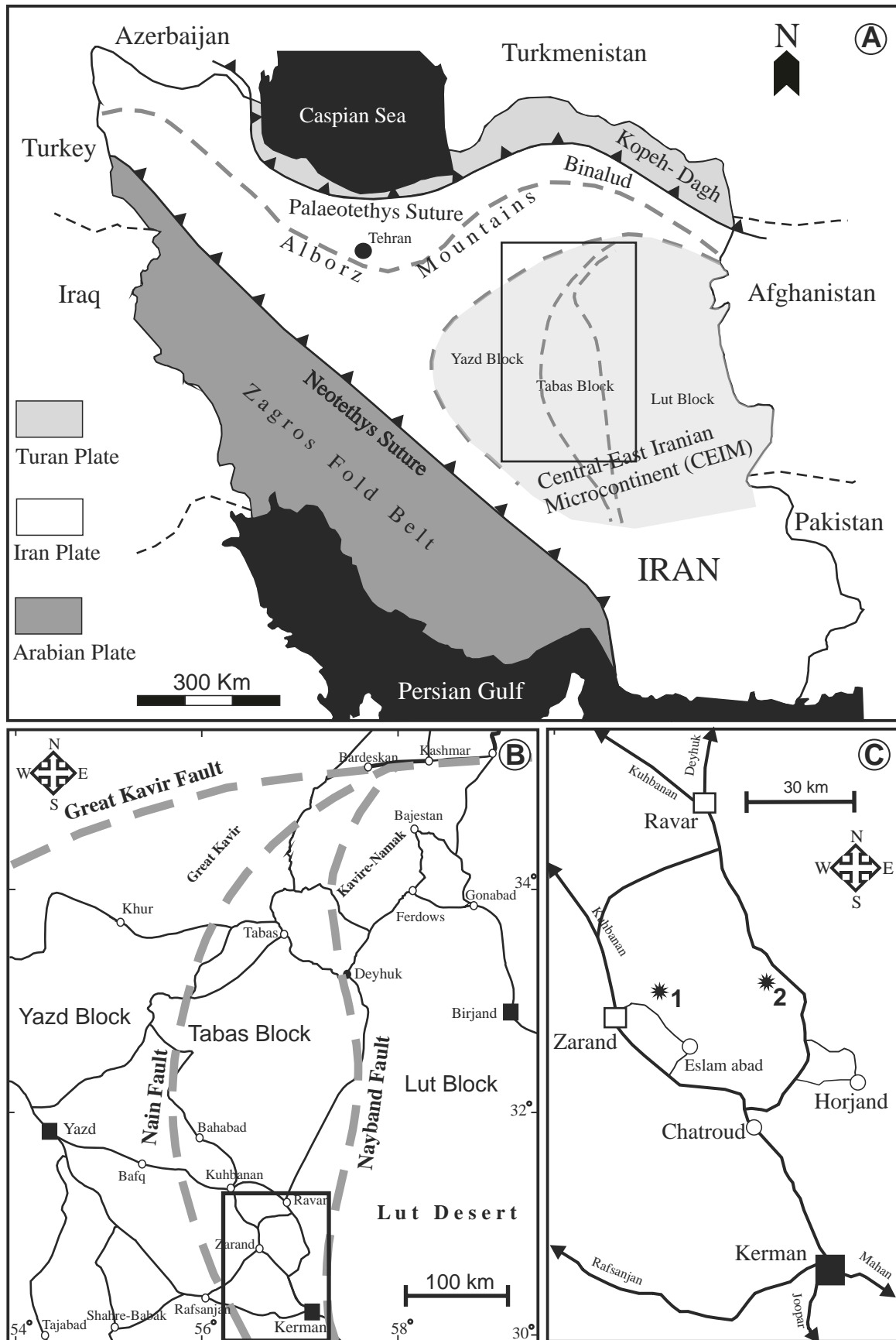
Figure 2. Location map of the study area and measured stratigraphic sections in SE central Iran. **A:** Present day map of Iran with the geographic domains and the main sutures and tectonic structures of the Iranian Plate (modified from Takin 1972 and Wilmsen et al. 2009). **B:** Close-up view of the rectangle in A, east-central Iran (modified from Wilmsen et al. 2010). **C:** Close-up view of the rectangle in B with the location of the measured sections in north Kerman, 1: Gazuieh section, 2: Sarashk section.
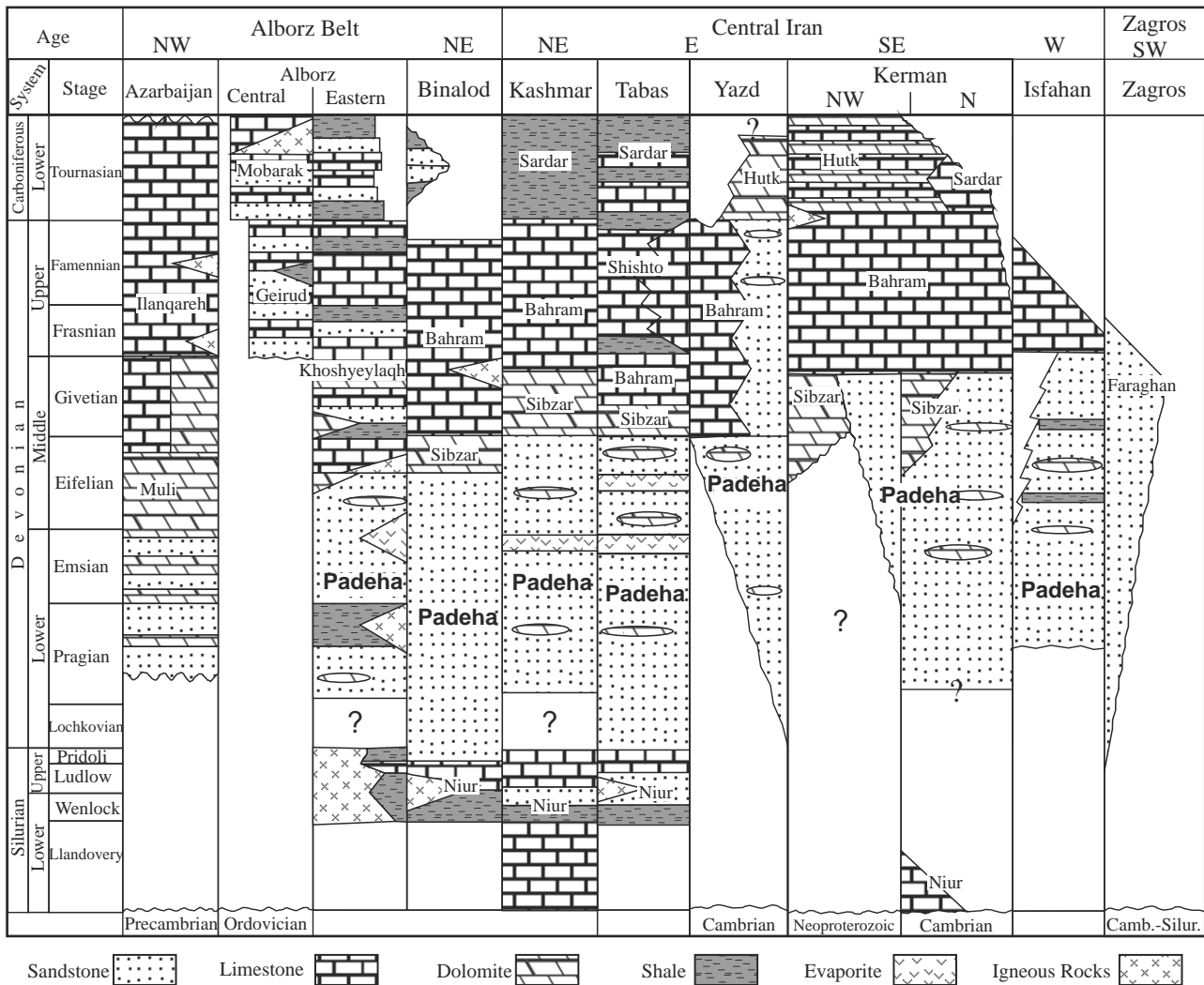
Figure 3. Lithostratigraphy (formations) and spatial-chronostratigraphic distribution of Devonian rocks in Iran (modified from Wendt et al. 2002, 2005).

systems from the Precambrian up to the Recent. The Tabas Block is bounded by the Great Kavir Fault in the north, the Naini Fault (Nain-Baft Fault) in the west and southwest and the Nayband Fault in the east (Fig. 2B). An important characteristic of the Block is that it bears a complete succession of Paleozoic rocks that is incomplete in other parts of Iran (Huckriede et al. 1962, Ruttner et al. 1968, Stocklin 1968). The present study focuses on the Early-Middle Devonian sandstones of the Padeha Formation in Gazuieh (East of Zarand) and Sarashk (75 km along the Kerman-Ravar road), north of Kerman in the southern part of the Tabas Block (Fig. 2C). Type and reference sections of the Padeha Formation in Ozbak-Kuh and Deranjal mountains respectively were introduced by Ruttner et al. (1968). In this area, the lower and upper boundaries of the Padeha Formation are transitional with coral limestones of the Niur Formation below and dolomites of the Sibzar Formation above, (Zand-Moghadam et al. 2013a). Facies patterns and sedimentary environments north of Kerman indicate a carbonate platform and a siliciclastic shelf during the Silurian to Middle Devonian and shallow open-marine embayment during the late Middle to Late Devonian, and a carbonate platform during the Early Carboniferous (Wendt et al. 2002, Zand-Moghadam et al. 2013b).

Based on Wendt et al. (2002) the Padeha Formation north of Kerman represents nearshore and delta environments in which cross beddings, symmetrical ripples and occasional mud cracks reflect extremely shallow water with possible fluvial intercalations. In restricted areas along the eastern margin of this shelf, intercalations of gypsum indicate local sabkha conditions (Zand-Moghadam et al. 2013b). More commonly, the Padeha Formation in the Kerman area is underlain by red siliciclastics and dolomites of Cambrian and sometimes Ordovician ages and overlain by fossiliferous limestone of the Bahram Formation of late Middle to Upper Devonian age (see Huckriede et al. 1962, Dimitrivic 1973, Wendt et al. 2002). The pre-Devonian hiatus, which comprises a time span in the order of up to 100 Ma, can be explained only by a widespread pre-Devonian emersion and erosion which spared a few areas with preserved Ordovician-Silurian remnants (Wendt et al. 2002).

METHODOLOGY

The Gazuieh section east of Zarand and the Sarashk section at km 75 on the Kerman-Ravar road were measured and sampled. For petrographic analysis, 320 thin sections were prepared and

Table 1. Detrital modes of 55 selected sandstone samples of the Padeha Formation. S indicates the Sarashk section and G the Gazuieh section. Qm non: Non-undulouse monocrystalline quartz; Qm un: Undulouse monocrystalline quartz; Qpq 2-3: Polycrystalline quartz (2-3 crystal units per grain); Qpq >3: Polycrystalline quartz (>3 crystal units per grain); Cht: Chert lithics; P: Plagioclase; K: Potassium feldspar; Lv: Volcanic fragments; Lm: Metamorphic fragments; Ls: Sedimentary fragments; Acc: Accessory minerals; Cem(T): Total cement in whole-rock sample. Values are given as percent of total grains.

Samples	Qm non	Qm un	Qpq 2-3	Qpq>3	K	P	Lv	Lm	Ls	Cht	ACC	Rock Type	Cem(T)	Sum
S1	75.9	23.9	0.0	0.0	0.0	0.0	0.0	0.0	0.0	0.0	0.2	Quartzarenite	8.3	280
S6	79.4	20.6	0.0	0.0	0.0	0.0	0.0	0.0	0.0	0.0	0.0	Quartzarenite	18.7	250
S8	88.4	10.3	0.0	0.0	0.0	0.0	0.0	0.0	0.0	1.2	0.1	Quartzarenite	4.4	300
S10	84.2	14.7	0.0	0.0	0.0	0.0	0.0	0.0	0.0	1.1	0.0	Quartzarenite	5.7	295
S12	71.0	26.6	0.0	0.0	0.0	0.0	0.0	0.0	0.0	2.1	0.3	Quartzarenite	7.9	275
S14	75.8	24.2	0.0	0.0	0.0	0.0	0.0	0.0	0.0	0.0	0.0	Quartzarenite	4.6	260
S16	78.2	20.4	0.0	0.0	0.0	0.0	0.0	0.0	0.0	1.4	0.0	Quartzarenite	5.3	280
S18	73.9	25.0	0.0	0.0	0.0	0.0	0.0	0.0	0.0	1.1	0.0	Quartzarenite	8.7	290
S21	74.4	23.3	0.0	0.0	0.0	0.0	0.0	0.0	0.0	2.3	0.0	Quartzarenite	12.3	270
S23	77.2	22.8	0.0	0.0	0.0	0.0	0.0	0.0	0.0	0.0	0.0	Quartzarenite	8.2	290
S25	69.8	28.7	0.0	0.0	0.0	0.0	0.0	0.0	0.0	1.1	0.4	Quartzarenite	3.9	300
S27	73.9	22.7	0.0	1.3	0.0	0.0	0.0	0.0	0.0	2.1	0.0	Quartzarenite	8.5	295
S30	62.4	35.2	0.0	0.0	0.0	0.0	0.0	0.0	0.0	2.2	0.2	Quartzarenite	7.8	260
S32	83.4	16.6	0.0	0.0	0.0	0.0	0.0	0.0	0.0	0.0	0.0	Quartzarenite	4.3	265
S34	72.2	26.6	0.0	0.0	0.0	0.0	0.0	0.0	0.0	1.1	0.2	Quartzarenite	13.6	270
S37	73.2	26.8	0.0	0.0	0.0	0.0	0.0	0.0	0.0	0.0	0.0	Quartzarenite	18.8	270
S40	68.4	30.5	0.0	0.0	0.0	0.0	0.0	0.0	0.0	1.0	0.1	Quartzarenite	5.1	290
S43	63.1	31.3	0.0	0.0	1.3	0.0	0.0	0.0	1.2	3.1	0.0	Sublitharenite	11.8	300
S49	65.3	22.0	0.8	5.0	0.0	0.0	0.0	0.0	0.0	6.9	0.0	Sublitharenite	13.9	300
S50	53.2	30.3	0.0	5.5	1.1	1.2	0.0	0.0	1.0	7.7	0.0	Sublitharenite	9.9	285
S56	69.0	15.9	0.0	4.3	0.0	0.0	0.0	0.0	0.0	10.8	0.0	Sublitharenite	7.8	270
S61	69.1	29.0	0.0	0.0	0.0	0.0	0.0	0.0	0.0	1.5	0.5	Sublitharenite	20.1	280
S66	70.7	21.0	0.0	3.1	0.0	0.0	0.0	0.0	0.0	5.2	0.0	Sublitharenite	5.1	295
S69	78.3	15.4	0.0	1.0	0.0	0.0	0.0	0.0	0.0	5.3	0.0	Sublitharenite	7.2	255
S71	83.2	13.6	0.0	0.0	0.0	0.0	0.0	0.0	0.0	3.1	0.1	Quartzarenite	4.9	280
S76	68.6	22.8	0.0	0.0	0.0	0.0	0.0	0.0	0.0	8.6	0.0	Sublitharenite	30.5	300
S117	69.0	26.8	0.0	0.0	0.0	0.0	0.0	0.0	0.0	3.5	0.7	Quartzarenite	14.5	300
S120	81.6	18.0	0.0	0.0	0.0	0.0	0.0	0.0	0.0	0.0	0.4	Quartzarenite	45.2	295
S122	76.6	20.9	0.0	0.0	0.0	0.0	0.0	0.0	0.0	2.1	0.4	Quartzarenite	5.1	255
S124	80.5	17.5	0.0	0.0	0.0	0.0	0.0	0.0	0.0	1.8	0.3	Quartzarenite	13.5	265
S127	80.6	15.7	0.0	0.0	0.0	0.0	0.0	0.0	0.0	3.5	0.2	Quartzarenite	15.7	260
S130	74.7	24.2	0.0	0.0	0.0	0.0	0.0	0.0	0.0	1.0	0.2	Quartzarenite	5.1	290
S135	76.8	20.0	0.0	0.0	0.0	0.0	0.0	0.0	0.0	3.1	0.1	Quartzarenite	4.8	285
G2	87.3	9.7	0.0	1.1	0.0	1.0	0.0	0.0	0.0	0.0	0.9	Quartzarenite	9.2	300
G5	85.9	10.3	0.0	2.1	0.0	0.0	0.0	0.0	0.0	1.1	0.6	Quartzarenite	3.9	295
G9	58.2	37.6	0.0	0.0	0.0	0.0	0.0	0.0	0.0	3.4	0.8	Quartzarenite	10.5	300
G15	23.2	69.7	0.0	0.0	0.0	1.8	0.0	0.0	0.0	4.6	0.7	Sublitharenite	34.7	300
G20	24.0	54.3	0.9	5.4	1.5	0.0	1.4	0.0	1.2	10.9	0.6	Sublitharenite	36.2	300
G25	13.3	73.4	0.6	2.3	1.1	2.6	0.0	0.0	0.0	6.7	0.0	Sublitharenite	24.8	300
G30	23.7	38.8	0.5	4.8	1.0	1.3	4.5	1.7	2.7	20.7	0.4	Litharenite	33.1	300
G34	31.4	46.2	0.0	0.0	5.1	8.2	0.0	0.0	0.0	8.5	0.7	Sublitharenite	40.4	300
G40	37.0	54.8	0.0	0.0	1.2	1.5	0.0	1.1	0.0	3.9	0.6	Sublitharenite	31.8	285
G44	31.3	51.6	0.0	0.0	2.6	5.3	0.0	0.0	0.0	8.5	0.8	Sublitharenite	27.4	295
G50	23.6	58.3	0.0	0.0	4.1	2.7	0.0	0.0	0.0	11.3	0.0	Sublitharenite	28.2	280
G55	40.6	45.4	0.0	0.0	1.3	0.0	0.0	0.0	0.0	12.2	0.5	Sublitharenite	19.5	300
G60	50.4	44.1	0.0	0.0	1.4	0.0	0.0	0.0	0.0	3.7	0.4	Quartzarenite	21.1	290
G71	51.3	31.1	0.0	4.8	0.0	0.0	4.2	0.0	0.0	8.1	0.6	Sublitharenite	37.8	295
G75	46.7	43.0	0.0	1.7	0.0	0.0	1.3	0.0	0.0	6.6	0.8	Sublitharenite	40.2	300
G80	28.1	51.9	0.0	0.0	0.0	1.3	4.1	0.0	0.0	13.7	1.0	Sublitharenite	27.8	300
G85	20.3	48.3	0.4	3.6	0.0	0.0	0.0	0.0	0.0	26.6	0.8	Litharenite	22.7	300
G91	28.6	54.7	0.0	5.1	0.0	0.0	0.0	0.0	0.0	10.6	1.0	Sublitharenite	23.4	290
G95	25.6	34.8	1.3	7.1	1.3	2.3	0.0	0.0	5.3	22.3	0.0	Litharenite	22.4	300
G104	63.9	22.9	0.9	2.0	0.0	0.0	0.0	0.0	0.0	9.5	0.8	Sublitharenite	29.4	295
G107	49.7	35.2	1.8	0.0	0.0	0.0	0.0	0.0	0.0	12.7	0.7	Sublitharenite	37.8	300
G112	72.1	19.8	0.0	0.0	0.0	0.0	0.0	0.0	5.4	1.9	0.9	Sublitharenite	44.6	300

studied with polarizing microscope. Petrofacies were named following the scheme of Folk (1980). Framework grains of fifty-five samples of sandstones were counted by considering 250 to 300 points per thin sections using the Gazzi–Dickinson method (Ingersoll et al. 1984; see Tables 1-2). The sediments mainly are well-sorted and fine- to medium-grained sandstones. Whole-rock chemical analyses were carried out on 20 sandstone samples which include sandstones with minimum carbonate, iron oxides and clay cement. Due to extensive carbonate and iron oxide cement in the sandstones of the Gazuieh section, samples were only selected from the Sarashk section for geochemical analyses. Analyses were carried out with the inductively coupled ICP-MS method at the commercial Acme Analytical Laboratories Ltd. in Vancouver, Canada, and the results are presented in Table 3.

RESULTS

Lithostratigraphy.- The Padeha Formation in the Kerman region is composed of sandstone, shale and scarce dolomite. In the Gazuieh section, this formation (Fig. 4) is 306 m thick and overlies Ordovician greenish shale. It is overlain by the Middle-Upper Devonian Bahram Formation. The Padeha Formation is commonly divided into four units. The first unit (126 m) is composed of sandstone-siltstone with sedimentary structures such as wavy ripple marks, interference ripple marks, cross-beds with bipolar pattern and bioturbation. The second unit (68 m) is mainly composed of red-purple shale with intercalations of red sandstone and conglomerate. The third unit (52.5 m) is composed of white sandstones (fining upwards cycles) associated with symmetrical ripples, reactivation surfaces and skolithos trace fossils. The upper unit (59.5 m)

Table 2. Point counting results of cement in the studied sandstones. S indicates the Sarashk section and G the Gazuieh section. Cem(T): Total cement in whole-rock sample; S.Cem: Silica cement; C.Cem: Carbonate cement; Fe.Cem: Iron oxide cement, Cl.Cem: Clay mineral cement. Except Cem(T); the remaining components are calculated from 100 percent of total cements.

Sample	Cem(T)	S.Cem	C.Cem	Fe.Cem	Cl.Cem	Sample	Cem(T)	S.Cem	C.Cem	Fe.Cem	Cl.Cem
S1	8.3	45.4	5.6	44.1	4.9	S122	5.1	93.4	0.0	5.4	1.2
S6	18.7	39.9	46.8	13.3	0.0	S124	13.5	31.2	20.7	25.5	22.6
S8	4.4	88.0	0.0	12.0	0.0	S127	15.7	13.1	21.2	20.6	45.1
S10	5.7	68.8	10.5	11.5	9.2	S130	5.1	95.7	0.0	4.3	0.0
S12	7.9	88.7	0.0	11.3	0.0	S135	4.8	91.4	0.0	8.6	0.0
S14	4.6	86.9	0.0	13.1	0.0						
S16	5.3	86.2	4.6	9.2	0.0	G2	9.2	5.2	65.1	20.5	9.2
S18	8.7	90.3	0.0	9.7	0.0	G5	3.9	7.8	0.0	82.4	9.8
S21	12.3	91.6	0.0	8.4	0.0	G9	10.5	15.3	35.2	24.1	25.4
S23	8.2	93.7	2.2	4.1	0.0	G15	34.7	9.8	14.3	30.1	45.8
S25	3.9	94.3	0.0	5.7	0.0	G20	36.2	8.1	19.5	37.5	34.9
S27	8.5	57.1	32.0	10.9	0.0	G25	24.8	18.3	5.4	71.5	4.8
S30	7.8	90.8	0.0	9.2	0.0	G30	33.1	3.8	14.6	27.9	53.7
S32	4.3	85.8	4.4	9.8	0.0	G34	40.4	0.0	42.5	12.9	44.6
S34	13.6	73.5	13.3	13.2	0.0	G40	31.8	0.0	4.9	11.7	83.4
S37	18.8	56.6	29.8	13.6	0.0	G44	27.4	5.6	55.2	4.2	35.0
S40	5.1	89.2	5.2	5.6	0.0	G50	28.2	9.2	30.1	9.4	51.3
S43	11.8	91.2	0.0	8.8	0.0	G55	19.5	52.3	43.9	3.8	0.0
S49	13.9	91.1	1.1	7.8	0.0	G60	21.1	4.3	26.8	66.2	2.7
S50	9.9	92.1	1.8	6.1	0.0	G71	37.8	34.7	43.9	21.4	0.0
S56	7.8	78.4	9.2	12.4	0.0	G75	40.2	43.8	37.9	18.3	0.0
S61	20.1	28.5	35.9	25.5	10.1	G80	27.8	13.9	6.8	75.8	3.5
S66	5.1	89.8	1.1	9.1	0.0	G85	22.7	23.9	32.1	36.2	7.8
S69	7.2	88.3	1.4	10.3	0.0	G91	23.4	43.6	34.3	22.1	0.0
S71	4.9	95.9	0.0	4.1	0.0	G95	22.4	28.7	28.5	42.8	0.0
S76	30.5	21.5	32.8	42.8	2.9	G104	29.4	0.0	92.6	7.4	0.0
S117	14.5	82.8	5.9	5.2	6.1	G107	37.8	0.0	72.3	24.5	3.2
S120	45.2	0.0	86.3	11.6	2.1	G112	44.6	0.0	88.4	7.3	4.3

consists of an alternation of sandstone, fine-crystalline dolomite, reddish shale and siltstone with symmetrical and asymmetrical ripples as well as mud cracks. In the Sarashk section (Fig. 4) the Padeha Formation is 297 m thick and has been divided into three units with purple sandstone (149 m) in the first unit, shale, evaporite and dolomite in the second unit (112 m) and white sandstone in the third unit (36 m). Sedimentary structures such as herringbone cross beds, hummocky cross beds, reactivation surfaces, symmetrical ripples and heterolithic layers with flaser, wavy and lenticular beddings are common in these units.

Petrography.- Most of the sandstones are fine to medium grain (0.05 to 1.30 mm); sub- to well rounded and well sorted. Monocrystalline quartz grains are abundant in the sandstone petrofacies (Fig. 5A, Table 1). In the Sarashk section, quartzarenite petrofacies dominate and the monocrystalline quartz often forms more than 90% of the detrial grains (83-100% with average 96.6). Sometimes, the quartz has inclusions of tourmaline. In the Gazuieh section, the abundance of monocrystalline quartz is lower (60-98% with an average of 92.9%), whereas the amount of polycrystalline quartz (0-8.4% with an average of 2.4%) and lithic grains (0-8.9% with an average of 1.7%) are higher. In the Gazuieh section, most of the petrofacies are sublitharenite and quartzarenite and few litharenite (chert arenite). The polycrystalline quartz exhibits smooth and suture borders (Fig. 5B). After quartz, chert is the most common grain. Its abundance in the Sarashk and Gazuieh sections is 11 and 27%, respectively. Chert grains mostly are microcrystalline (Fig. 5C) and sometimes chalcedony. In the Gazuieh section also volcanic (Fig. 5D), metamorphic, sandstone (Fig. 5E-F) and shale lithics are observed in the sandstones (Table 1). Feldspar in the sandstones is scarce and ranges from 0 to 4% (with few exceptions) of the total grains in the Gazuieh section and up to 2% in the Sarashk section (Table 1, Fig. 5G). Altered microcline and plagioclase are the main types of feldspar. Opaque grains, zircon and muscovite form less than 1% of total detrital grains (Table 1). The abundance of cement reaches up to 14% of the whole rocks and the average is 5 and 9% for Sarashk and Gazuieh sections, respectively.(Table 2). Cement types include silica, carbonate, iron oxide and clay minerals (especially chlorite); the amounts of cement in the sandstone in the Gazuieh section are much higher than those in the Sarashk section (see Table 2 and Fig. 5G-H).

Geochemistry.- The sandstones of the Padeha Formation have SiO_2 contents of 92-98% (Table 3). Weight percentual variations of Al_2O_3 and Fe_2O_3 are between 0.3 to 4 and 0.2 to 1.5, respectively, whereas other major oxides generally are below 1 wt. %. In comparison to the upper continental crust (UCC), all major elements are depleted, except for SiO_2 which shows enrichment. Values of indicative elemental ratios for provenance, such as Th/Sc (1.1-4.1), Th/Co (0.7-4.7), La/Sc (5.5-16.5) and La/Co (1.9-20.6) invariably are above those for the UCC (Table 4). The Zr/Sc ratio, which reflects the zircon content, sorting and recycling of sediments, ranges from 48 to 368. Th/U in sedimentary rocks is interesting for interpretation of palaeoweathering and recycling, ranging from 0.5 to 6.8 in
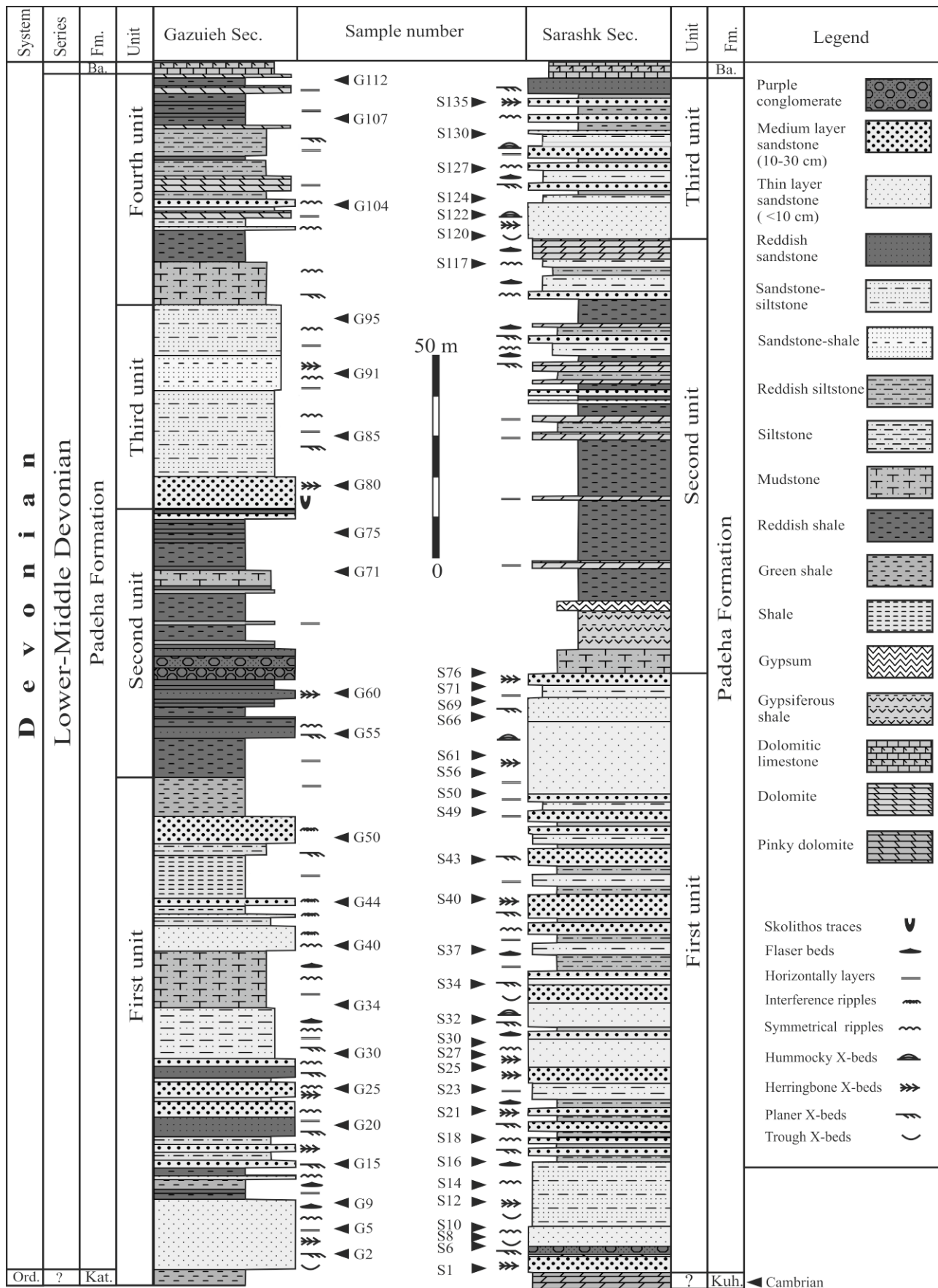
Figure 4. Log-sections of the Early-Middle Devonian Padeha Formation, Gazuieh (G) and Sarashk (S) sections. Sample numbers are indicated. Ord.: Ordovician; Kat: Katkuied Formation; Kuh: Kuhbanan Formation; Ba: Bahram Formation.
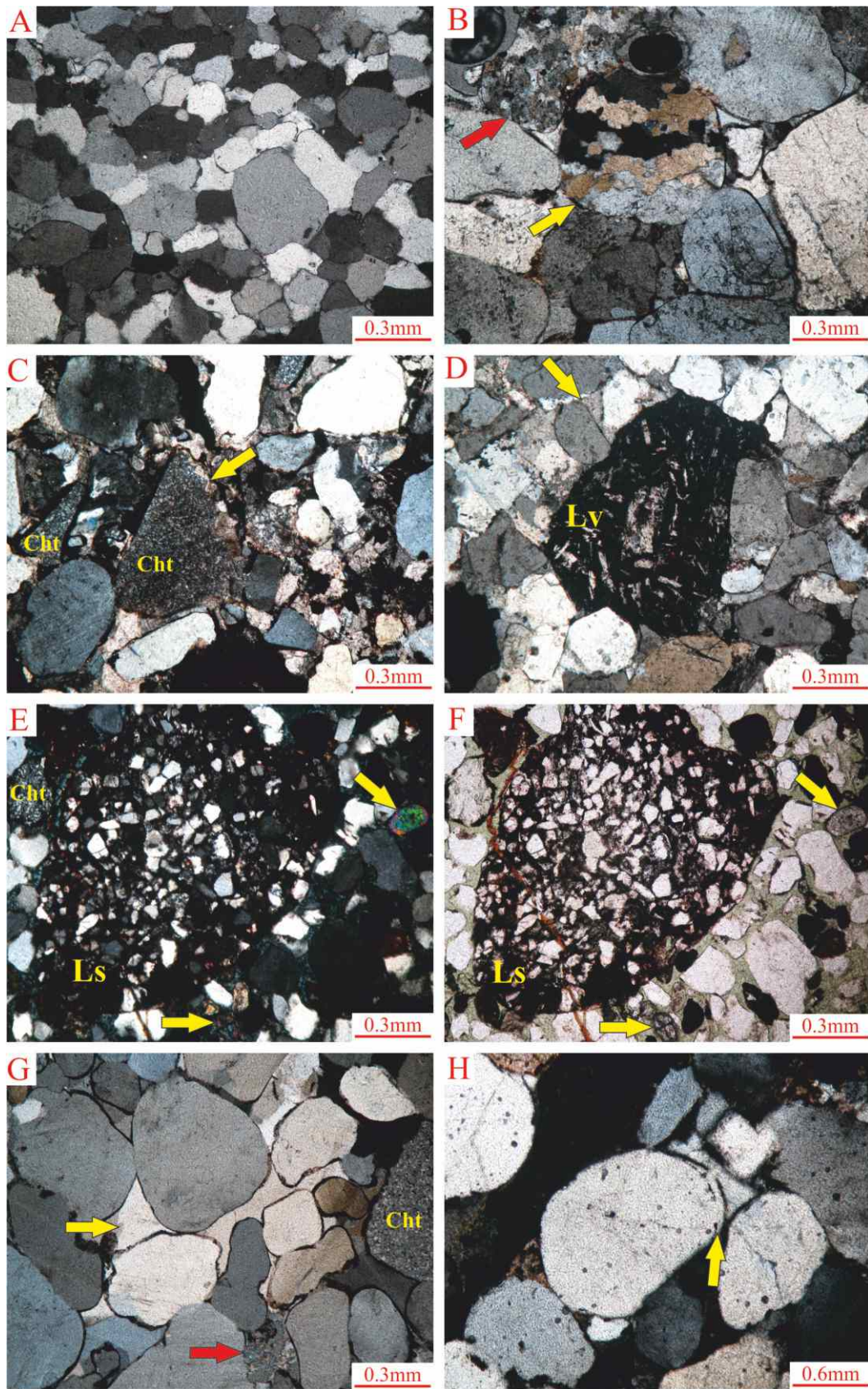
Figure 5. Photomicrographs of sandstones of the Padeha Formation. **A:** Monocrystalline quartz grains dominate, especially in the quartzarenites (sample S14). **B:** Polycrystalline quartz grains of metamorphic origin (yellow arrow) and plutonic origin (red arrow) in quartzarenite (sample G5). **C:** Chert grains (Cht) in litharenite (chertarenite). Some chert has been dissolved and replaced by carbonate (yellow arrow) (sample G85). **D:** Volcanic lithic fragment (Lv) surrounded by carbonate cement (yellow arrow) (sample G30). **E, F:** sandstone fragment (Ls) and rounded grains of zircon (yellow arrows) indicating recycling. The cement in this sample is chlorite (green color in F; sample G95). **G:** Pore-filling silica cement (dominant in the studied sandstones), yellow arrow. Red arrow indicates altered K-feldspar grain (G75). **H:** Overgrowth cement (yellow arrows) indicating recycling (G50). All images prepared with crossed-polarized light except for the plane-polarized light image in F.

Table 3. Elemental composition of the Padeha Formation sandstones from the Sarashk section. Oxides and loss of ignition (LOI) are in percentage and trace elements in ppm.

Sample	SiO₂	Al₂O₃	Fe₂O₃	MgO	CaO	Na₂O	K₂O	TiO₂	P₂O₅	MnO	Cr₂O₃	LOI	Th	U	Sc	Zr
S12	96.92	1.31	0.42	0.05	0.26	0.01	0.38	0.12	0.02	0.009	0.008	0.5	1.9	0.7	1	253.4
S14	96.92	1.23	0.35	0.07	0.22	0.008	0.34	0.07	0.01	0.006	0.008	0.8	1.9	0.3	0.9	86.3
S18	97.64	0.78	0.60	0.03	0.08	0.005	0.20	0.07	0.03	0.008	0.006	0.6	1.0	0.4	0.8	152.3
S21	96.80	0.38	0.33	0.04	1.18	0.009	0.09	0.02	0.02	0.007	0.005	1.2	0.8	0.3	0.7	33.0
S25	98.10	0.51	0.34	0.02	0.28	0.006	0.14	0.03	0.03	0.005	0.009	0.6	0.8	0.4	0.9	58.7
S30	98.05	0.55	0.55	0.03	0.20	0.008	0.14	0.07	0.02	0.008	0.010	0.4	1.2	0.6	0.8	196.3
S34	98.00	0.36	0.51	0.02	0.53	0.009	0.08	0.02	0.02	0.005	0.007	0.5	0.9	0.2	0.7	33.6
S40	97.96	0.90	0.35	0.04	0.09	0.007	0.24	0.06	0.04	0.008	0.009	0.3	1.4	0.5	0.8	121.7
S43	97.97	0.89	0.49	0.04	0.06	0.01	0.23	0.05	0.03	0.006	0.009	0.3	1.0	0.4	0.6	85.3
S49	95.29	2.42	0.52	0.09	0.07	0.007	0.69	0.06	0.05	0.007	0.005	0.8	2.2	0.5	0.7	108.3
S50	97.51	0.80	0.48	0.04	0.19	0.005	0.19	0.04	0.03	0.005	0.009	0.7	0.9	0.4	0.8	84.7
S56	94.65	1.76	0.67	0.09	0.98	0.008	0.50	0.11	0.02	0.008	0.015	1.2	2.0	0.7	0.7	258.1
S66	97.70	0.36	0.52	0.02	0.03	0.009	0.07	0.03	0.02	0.05	0.011	1.3	1.2	0.4	0.6	59.1
S69	97.52	0.63	0.87	0.04	0.24	0.005	0.15	0.04	0.03	0.01	0.016	0.5	0.9	0.4	0.8	88.9
S71	98.05	0.82	0.40	0.03	0.08	0.008	0.21	0.04	0.02	0.005	0.008	0.4	1.0	0.3	0.9	76.5
S117	94.47	2.31	0.60	0.29	0.35	0.006	0.59	0.10	0.03	0.009	0.011	1.2	2.9	1.8	0.7	112.7
S122	96.26	1.23	0.28	0.04	0.76	0.01	0.29	0.05	0.02	0.006	0.015	1.0	1.4	0.9	0.9	64.6
S127	91.53	4.14	1.58	0.12	0.11	0.05	0.96	0.23	0.03	0.008	0.024	1.2	6.2	0.9	1	222.1
S130	96.89	0.67	0.56	0.04	0.41	0.009	0.11	0.05	0.02	0.009	0.023	0.7	1.3	1.1	0.9	66.8
S135	97.74	0.74	0.41	0.03	0.04	0.006	0.16	0.08	0.01	0.007	0.016	0.8	1.0	1.9	0.7	250.2

Sample	Co	La	Ce	Pr	Nd	Sm	Eu	Gd	Tb	Dy	Ho	Er	Tm	Yb	Lu
S12	0.4	5.6	8.9	1.15	3.3	0.64	0.10	0.54	0.09	0.57	0.18	0.72	0.07	0.53	0.10
S14	0.1	9.5	18.0	1.96	7.8	0.85	0.15	0.57	0.07	0.55	0.06	0.46	0.06	0.29	0.06
S18	0.2	4.5	8.0	0.96	2.7	0.64	0.07	0.51	0.06	0.49	0.07	0.31	0.04	0.22	0.06
S21	0.1	4.8	8.2	1.00	2.8	0.70	0.10	0.43	0.06	0.16	0.04	0.23	0.03	0.15	0.01
S25	0.2	5.9	8.4	1.18	3.3	1.12	0.17	0.61	0.08	0.47	0.06	0.38	0.04	0.20	0.05
S30	0.3	6.2	10.5	1.31	5.7	0.89	0.13	0.60	0.11	0.50	0.09	0.41	0.09	0.73	0.08
S34	0.8	9.6	8.4	0.91	2.9	0.28	0.06	0.22	0.06	0.32	0.06	0.21	0.02	0.18	0.03
S40	0.1	6.1	11.3	1.36	6.2	0.95	0.18	0.82	0.14	0.72	0.14	0.28	0.04	0.37	0.04
S43	0.8	5.2	7.8	1.09	3.6	0.53	0.16	0.69	0.08	0.54	0.08	0.34	0.05	0.29	0.03
S49	0.6	11.6	19.1	3.03	12.3	2.50	0.49	1.53	0.20	0.97	0.15	0.35	0.04	0.55	0.07
S50	0.9	5.6	9.4	1.45	4.7	1.10	0.16	0.85	0.13	0.74	0.15	0.36	0.03	0.19	0.04
S56	1.0	5.6	8.8	1.10	4.2	0.70	0.21	0.76	0.13	0.56	0.15	0.57	0.09	0.47	0.11
S66	0.3	5.8	9.5	1.19	3.8	0.84	0.11	0.63	0.07	0.27	0.08	0.26	0.02	0.26	0.04
S69	1.1	4.4	7.6	0.96	3.3	0.36	0.07	0.43	0.07	0.36	0.05	0.20	0.02	0.16	0.05
S71	0.4	5.0	9.4	1.19	6.7	0.68	0.06	0.43	0.08	0.41	0.09	0.36	0.03	0.45	0.05
S117	4.0	7.9	15.2	1.88	6.5	1.14	0.15	0.81	0.12	0.68	0.14	0.35	0.05	0.25	0.06
S122	0.3	5.9	10.3	1.28	4.4	0.61	0.12	0.44	0.06	0.35	0.08	0.26	0.04	0.24	0.05
S127	2.6	11.4	18.7	2.05	7.3	1.05	0.20	0.92	0.19	1.17	0.24	0.85	0.13	0.97	0.16
S130	0.7	5.2	8.3	0.93	2.9	0.62	0.07	0.59	0.08	0.48	0.10	0.28	0.04	0.21	0.05
S135	0.5	4.8	9.0	1.13	4.0	0.46	0.05	0.39	0.05	0.46	0.13	0.37	0.06	0.42	0.08

the sandstones of the Padeha Formation. Chondrite-normalized rare earth element (REE) concentrations generally are lower than those of the UCC (Fig. 6) but with similar trends. The light REE/heavy REE ratio is positive and Eu has negative anomalies.

DISCUSSION AND CONCLUSION

Petrography.- Qualitative petrographic studies may provide information on the nature of the source area (Weltje and von Eynatten 2004). Several petrographical techniques for determination of sandstone provenance exist (e.g. Wanas & Abdel-Maguid 2006), but investigation of the undulosity and polycrystallinity of quartz grains (Basu et al. 1975, Young 1976) is also common (e.g. Jafarzadeh & Hosseini-Bazri 2008, Najafzadeh et al. 2010, Khanehbad et al. 2012). Because of the scarcity of feldspar and rock fragments, our provenance investigations are based on the interpretation of quartz grain types. The dominance of non-undulatory monocrystalline grains is in accordance with mainly middle to upper rank metamorphic quartz for the Sarashk Section (Fig. 7A). In the Gazuieh section the higher content of undulatory monocrystalline quartz points to mainly low to middle rank metamorphic parent rocks. Quartzarenites can be derived from several origins (Suttner et al. 1981) and characteristics of

quartz grains and accessory minerals mostly can be used for source rock interpretations of quartzarenite.

The abundance of monocrystalline quartz with small amounts of feldspars can be due to severe chemical weathering in the source area, long distance transport or high-energy depositional environment (Suttner et al. 1981, Amireh 1991, Wanas & Abdel-Majuid 2006). According to Dabbagh and Rogers (1983) relatively high proportions of fine- to medium-grained monocrystalline quartz in sandstones may be attributed to the disaggregation of original polycrystalline quartz during high energy and/or long distance transport from the source area. Polycrystalline quartz grains with straight to slightly curved intercrystalline boundaries, monocrystalline quartz grains with straight extinction associated with inclusions of tourmaline and accessory minerals such as zircon and muscovite in the studied sandstones indicate that plutonic rocks may have been the main source for the Padeha Formation (e.g. Blatt et al. 1980, Morton et al. 1992, Ahmad & Bhat 2006, Zaid 2012), but the existence of suture intercrystalline boundaries of polycrystalline quartz grains and volcanic lithics also show subordinate metamorphic and mafic volcanic source rocks, respectively. Sandstones from different tectonic settings have different detrital components (Dickinson et al. 1983, Yan et al. 2006).

In general, four major tectonic provenance types, stable

Table 4. Range of elemental ratios of the sandstones of the Padeha Formation from the Sarashk section compared with elemental ratios in similar fractions derived from felsic and mafic rocks and the upper continental crust.

Elemental Ratio	UCC*	Range of sediment from mafic rocks**	Range of sediment from felsic rocks**	Range of sandstone from Padeha Fm.
La/Sc	2.21	0.43-0.86	2.50-16.30	5.50-16.57
Th/Sc	0.79	0.05-0.22	0.84-20.50	1.12-4.14
La/Co	1.76	0.14-0.38	1.80-13.80	1.97-20.66
Th/Co	0.63	0.04-1.40	0.67-19.40	0.72-4.75

* Taylor & McLennan (1985), McLennan (2001); ** Cullers et al. (1988), Cullers (2000), Cullers & Podkovyrov (2000).

cratons, basement uplifts, magmatic arcs, and recycled orogen, can contribute to the composition of detrital grains in sandstones (Dickinson & Suczek 1979, Dickinson et al. 1983). The high quartz content is in accordance with stable craton interior and slightly recycled orogen provenances for both sections (particularly in the Gazuieh section, Fig. 7B). This would mean that the mature Padeha Formation sandstones derived from relatively low relief granitoid and gneissic sources, supplemented by recycled sands from associated platform or passive margin basins (see Dickinson et al. 1983). These interpretations are supported by medium to fine-grained, sub-rounded to well-rounded and well-sorted quartz. Furthermore, recycled quartz grains and well-rounded zircon indicate several phases of recycling and extensive reworking conditions from a cratonic or a recycled source. However, processes of diagenesis may change the original composition of the rocks (McBride 1985). Hence, petrographic determination must be considered with caution.

Geochemistry.- Geochemical data of sandstones can be complementary for petrographic data and would help in determining the source characteristics (e.g. Bhatia 1983, Roser & Korsch 1988). Based on major oxides in sandstones, Schwab (1975), Bhatia (1983), Roser and Korsch (1986, 1988) and Armstrong-Altrin et al. (2004) suggested several discriminant-function diagrams that can be used to understand the provenance. The major element composition shows that the studied sandstones may be derived from mature polycyclic continental sedimentary rocks (Fig. 8A). Different to the major elements, some trace elements and all REE are considered to be immobile under diagenesis, metamorphism and alteration; therefore, immobile elements are commonly used in provenance and tectonic setting interpretation (e.g. Bahlburg 1998, Zimmermann & Bahlburg 2003, Augustsson & Bahlburg 2008). Mafic and felsic source rocks differ significantly in the ratios such of La/Sc, Th/Sc, La/Co and Th/Co and hence provide useful information about the provenance of siliciclastic sedimentary rocks (see Cullers 2000; Cullers & Podkovyrov 2000). In the present study La/Sc, Th/Sc, La/Co and Th/Co values of the Padeha Formation sandstones are more similar to values for sediments derived from felsic source rocks than those from mafic source rocks, thus suggesting felsic source rocks (Table 4). The Th/U ratio in most upper crustal rocks typically ranges between 3.5 and 4 and values higher than 4 may indicate intense weathering in the source areas or sediment recycling (McLennan et al. 1993). Therefore the generally high Th/U for the Padeha Formation sandstones indicates the derivation of these sandstones from recycling of the continental crust. Sc and Th are transferred quantitatively

from source to sediment; hence, the ratio is used to deduce the composition of the source rock (McLennan et al. 1993). The Zr/Sc ratio is considered as one of the proxy to evaluate the presence or absence of recycling (McLennan et al. 1993). The recycled source rocks for most samples from Sarashk section are supported both by their high Th/Sc and Zr/Sc ratio (Fig. 8B).The REE pattern and the Eu anomaly can be useful for determination of source rocks (Taylor & McLennan 1985). Based on Cullers et al. (1987), felsic igneous rocks usually contain higher LREE/HREE ratios and negative Eu anomaly and basic igneous rocks contain low LREE/HREE ratios and little or no Eu anomalies. In the Padeha Formation sandstones, higher LREE/HREE ratios, negative Eu anomaly, and similar trend of chondrite normalized REE pattern with UCC (Fig. 6) suggest that the Padeha Formation sandstones derived from an old UCC composed chiefly of felsic components. According to Bhatia (1985), sediments deposited on passive continental margins have LREE enrichment, negative Eu anomaly and flat HREE in the chondrite-normalized rare earth element patterns. Thus, the REE patterns support the passive continental margin for Padeha Formation sandstones in the Sarashk section.

Implications for palaeogeography

Palaeogeographic maps of the Late Ordovician to Late Devonian of northern Arabia suggest that north Africa and Arabia formed a broad stable continental shelf on the northern margin of the Gondwana supercontinent (Husseini 1991, Sharland et al. 2001, Ruban et al. 2007, Torsvik & Cocks 2009) bordering the Paleo-Tethys Ocean. The Iran plate with a collection of smaller blocks of probable Gondwanan or peri-Gondwanan affinity are considered as parts of the Cimmerian continent during evolution of the Paleo-Tethys and Neo-Tethys
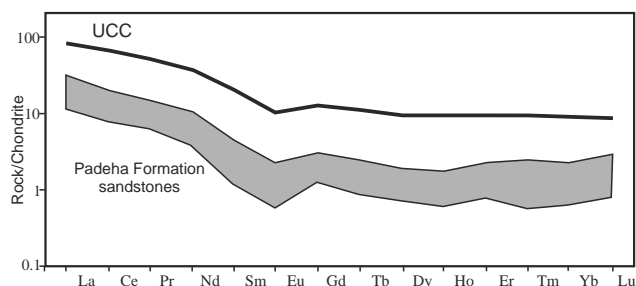
Figure 6. Chondrite-normalized REE patterns for samples of the sandstones of the Padeha Formation. Chondrite values are from Taylor and McLennan (1985).
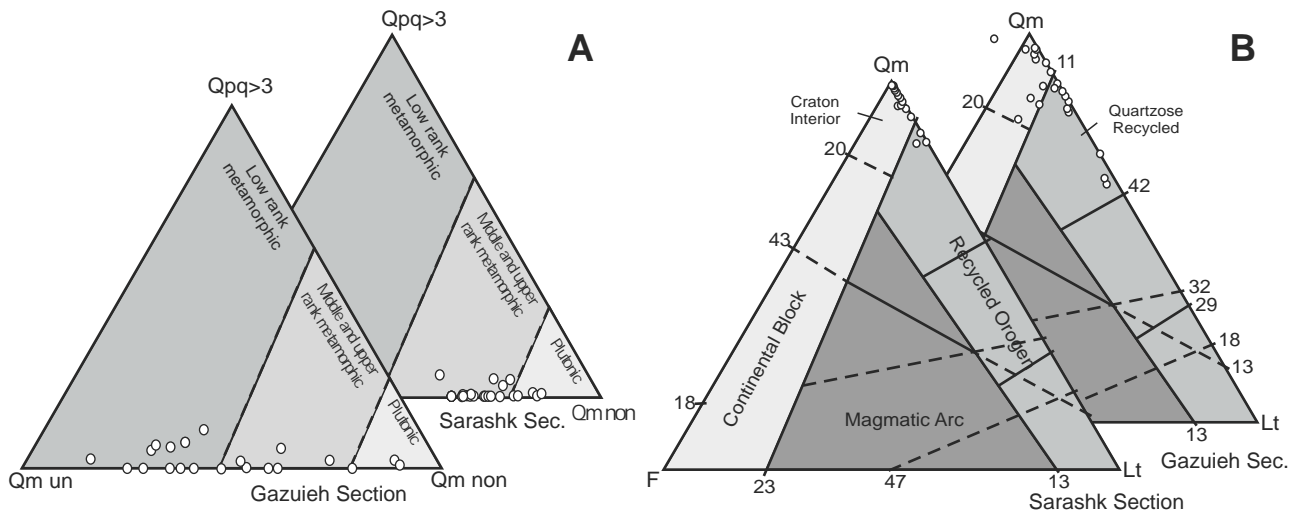
Figure 7. Diagrams of petrography for provenance of the Padeha Formation sandstones. **A:** Quartz grain varieties plotted on the Basu et al. (1975) diagram. Qm non: Non-unduloose monocrystalline quartz; Qm un: Unduloose monocrystalline quartz; Qpq >3: Polycrystalline quartz (>3 crystal units per grain). **B:** Qm-F-Lt ternary diagrams of tectonic setting for the studied sandstones based on Dickinson et al. (1983). Qm: Monocrystalline quartz; F: feldspar; Lt: Siliciclastic lithic fragments.

oceans (Sengör 1987, Ruban et al. 2007; Fig. 9). From the Late Ordovician to the Late Devonian, the Iranian terranes, including Central Iran, Alborz and Sanandaj-Sirjan, had peri-Gondwanan/Gondwanan position and were located at 15-30°S palaeolatitude (Cocks & Torsvik 2002).

This paleotropical latitude implying humid to semi-humid climate is supported by high quartz and low Al_2O_3 content in the sandstones of the Padeha Formation. Most studies consider that the Paleozoic successions of Iran represent shallow-marine passive margin sedimentation with no significant magmatism or deformation (Stocklin 1968, Berberian & King 1981, Lasemi 2001, Wendt et al. 2002, 2005) so that submarine volcanic rocks at the base of the Niur Formation in the northern Tabas Block and Silurian basalts in Alborz mountains (Soltan Meydan Formaton) are attributed to the start of an intracontinental passive rifting phase in the Late Ordovician to Early Silurian (Berberian & King 1981, Stampfli et al. 1991, Lasemi 2001).

The fining upward cycles of sandstone with symmetrical and interference ripple marks, herringbone and hummocky cross beds, reactivation surfaces, flaser, wavy and lenticular beddings, mud cracks and mature quartzarenite petrofacies show that the Padeha Formation in the studied area was deposited in a coastal environment, mainly under a tidal flat setting. In the upper tidal flat, the reddish shale and evaporite facies established in a marine sabkha environment (Klein 1971, 1998, Khalifa et al. 2006, Warren 2006, Chakraborty & Sensarma 2008, Zand-Moghadam et al. 2009, Longhitano et al. 2012, Zand-Moghadam et al. 2013b). This interpretation is similar to that of Wendt et al. (2002; discussion above). Thus, the Padeha Formation sandstones support sedimentation may have taken place in shoreline to shallow marine passive continental margin conditions. Lasemi (2001) suggested that a failed rift basin in the Tabas Block formed during the Early Ordovician at the margin of Paleo-Tethys in the northern parts of Central Iran. Based on paleocurrent analyses of the Padeha
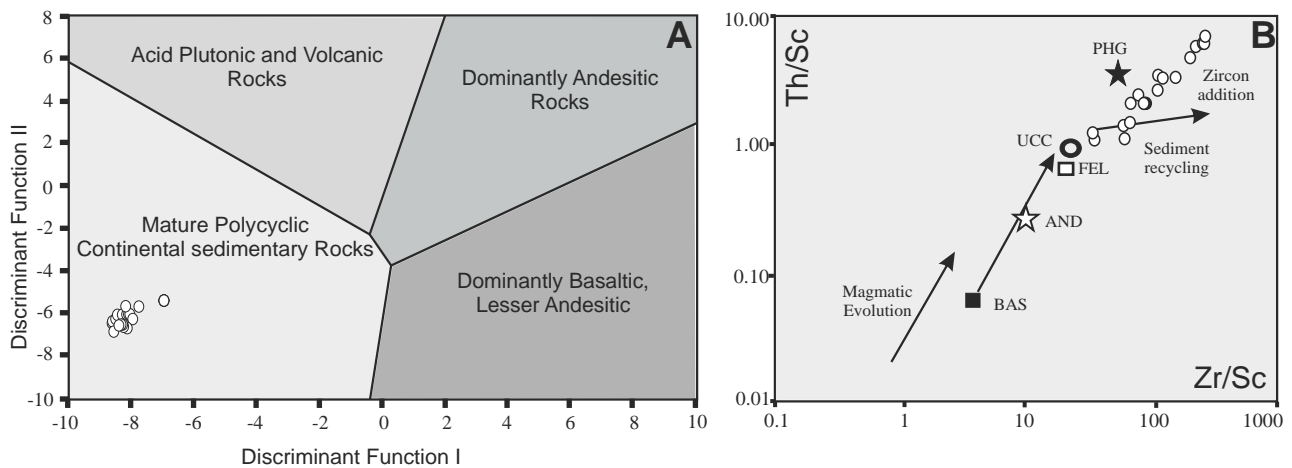
Figure 8. Diagrams of geochemistry for provenance of the Padeha Formation sandstones. **A:** Major element Discriminant Function diagram of Roser & Korsch (1988) for the Sarashk section. **B:** Th/Sc versus Zr/Sc diagram (modified after McLennan et al. 1993). PHG (Phanerozoic granite), FEL (felsic volcanic rock), AND (andesite), BAS (basalt), UCC (Upper Continental Crust).
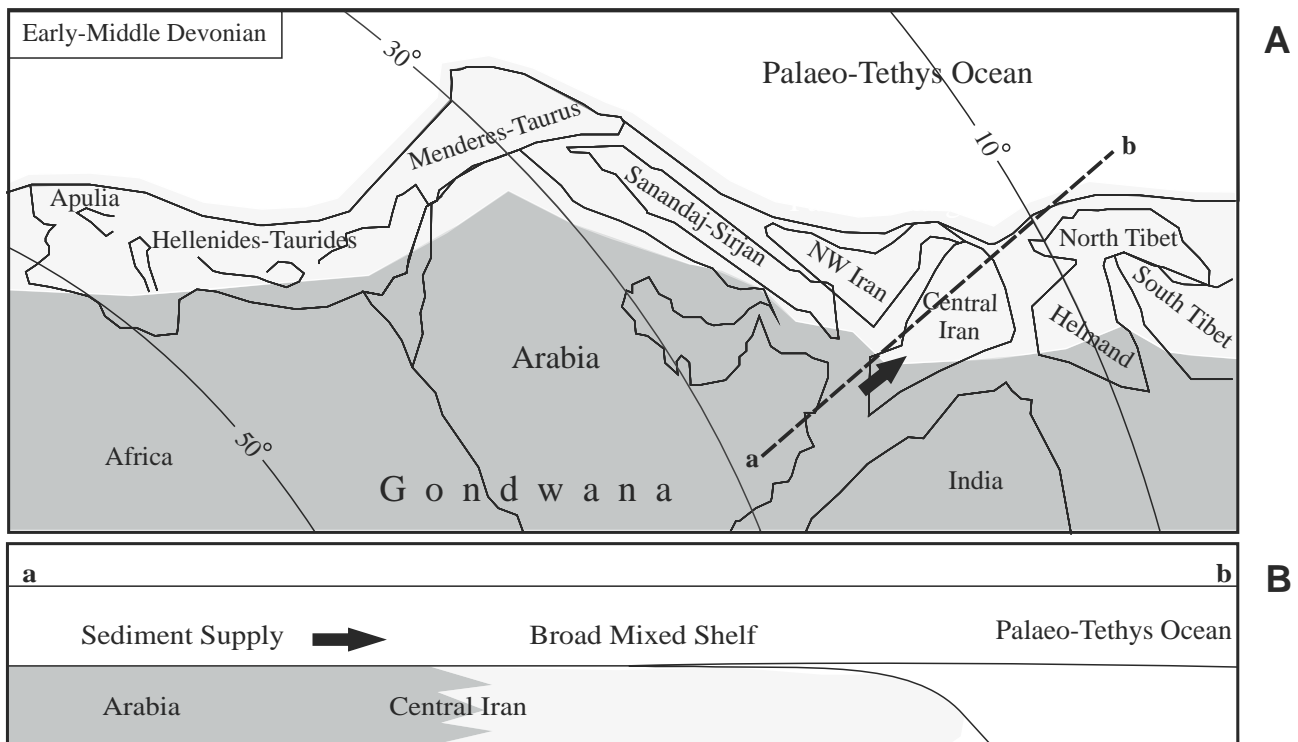
Figure 9. Palaeogeographic map (**A**) and schematic plates cross-section (**B**) of the Central Iran and adjoining micro-plates during the Early-Middle Devonian; modified from Ruban et al. (2007) after results of the present study. The transect a-b indicated in **A** is represented in **B**.

Formation (Zand-Moghadam et al., 2013a,b), and palaeogeography maps (e.g. Husseini 1991, Lasemi 2001, Ruban et al. 2007), this failed rift basin was a path for sediment transport into the ocean and likely the Padeha siliciclastic rocks were transported through this path from the south and southwest of Central Iran toward the north and northeast into the margin of Palaeo-Tethys.

The restriction of a carbonate regime in Central Iran and facies differences in the Silurian deposits as well as volcanic rocks of Silurian age have been attributed to a syn-rift phase for the Paleo-Tethys margin (Lasemi 2001). Aharipour et al. (2010) studied the Padeha Formation in the Eastern Alborz Mountains and stated that the rocks were deposited in three terrestrial environments (alluvial fan, distal fan, and palustrine/lacustrine) interpreted as syn-rift deposits. During the Early to Middle Devonian, Central Iran was a place for mixed siliciclastics and carbonate sedimentation along the coastal setting and the shallow marine environments (Wendt et al. 2002, 2005). In the paleogeographic maps of the Middle East for the Devonian (e.g. Ruban et al. 2007, Torsvik & Cocks 2009, Hairapetian et al. 2011), Central Iran is shown as a separate terrane as well as detached from the Arabian plate (Fig. 9).

Our field observations such as (1) rocks overlain the Padeha Formation with different ages in different parts of Iran (Figs. 3-4), (2) volcanic, metamorphic and sedimentary lithic fragments, (3) the dominance of quartzarenitic petrofacies (Table 1), (4) geochemical data (Figs. 6 and 8), and (5) paleogeography (Fig. 9), show that the Padeha Formation sandstones may have been derived from felsic and mature recycled rocks into the cratonic interior. On the other hand, these sandstones would have been deposited in a continental embankment in the passive margin along the southern Palaeo-Tethys. It is possible that in Central Iran have formed a horse-graben system as a failed rift in Early to Late Paleozoic, with normal faults (Lasemi, 2001). In this framework sediments would have been removed from high areas and deposited in grabens along the Palaeo-Tethys ocean. Therefore, based on present results showing differences in the petrofacies of two sections, we assume that the source of the Padeha Formation sandstones might have been from different uplifts, as a horse type, and have been deposited in the Central Iran and Tabas Block.

There are no available data constraining the age of our source sediments, but we have shown that there was likely a short dispersal path between the source area and depocenter during deposition of the Padeha Formation (erosion of the pre-rift and syn-rift sedimentary substratum) as shown by the paleocurrent analyses (Zand-Moghadam et al. 2013a, b). It seems that local extensions of the rifted basins in the Tabas block can be attributed to small basins that need further consideration for tectonic and sedimentation studies.

REFERENCES

Aharipour R., Moussavi M.R., Mosaddegh H. & Mistiaen, B., 2010. Facies features and paleoenvironmental reconstruction of the Early

to Middle Devonian syn-rift volcano-sedimentary succession (Padeha Formation) in the Eastern-Alborz Mountains, NE Iran. *Facies* **56**: 279-294.

Ahmad A.H.M. & Bhat G.M., 2006. Petrofacies, Provenance and diagenesis of the dhosa sandstone member (Chari Formation) at Ler, Kachchh sub-basin, Western India. *Journal of Asian Earth Sciences* **27**: 857-872.

Al-Hajri S.A. & Filatoff J., 1999. Stratigraphy and operational palynology of the Devonian System in Saudi Arabia. *GeoArabia* **4**: 53-68.

Al-Juboury A.I. & AL-Hadidy A.H., 2009. Petrology and depositional evolution of the Paleozoic rocks of Iraq. *Marine and Petroleum Geology* **26**: 208-231.

Al-Sharhan A.S. & Nairn A.E.M., 1997. Sedimentary Basins and Petroleum Geology of the Middle East. 843 p., Amsterdam.

Amireh B.S., 1991. Mineral composition of the Cambrian–Cretaceous Nubian Series of Jordan: provenance, tectonic setting and climatological implication. *Sedimentary Geology* **71**: 99–119.

Armstrong-Altrin J.S., Lee Y.I., Verma S.P. & Ramasamy, S., 2004. Geochemistry of sandstones from the Upper Miocene Kudankulam Formation, southern India: implication for provenance, weathering and tectonic setting. *Journal of Sedimentary Research* **74**: 285-297.

Augustsson C. & Bahlburg, H., 2008. Provenance of late Palaeozoic metasediments of the Patagonian proto-Pacific margin (southernmost Chile and Argentina). *International Journal of Earth Sciences* **97**: 71-88.

Bahlburg H., 1998. The geochemistry and provenance of Ordovician turbidites in the Argentine Puna. *In*: Pankhurst R.J. and Rapela C.W. (*eds*.): The Proto-Andean Margin of Gondwana. *Geological Society of London Special Publication* **142**:127-142.

Basu A., Young S.W., Suttner L.J., James W.C. & Mack, G.H., 1975. Re-evaluation of the use of adulatory extinction and polycrystallinity in detrital quartz for provenance interpretation. *Journal of Sedimentary Petrology* **45**: 873-882.

Berberian M. & King G.C.P., 1981. Toward a palaeogeography and tectonic evolution of Iran. *Canadian Journal Earth Sciences* **18**: 210-265.

Bhatia M.R., 1983. Plate tectonics and geochemical composition of sandstones. *Journal of Geology* **91**: 611-627.

Bhatia M.R., 1985. Plate tectonics and geochemical composition of sandstones: a reply. *Journal of Geology* **93**: 85–87.

Blatt H., Middleton G. & Murray R., 1980. Origin of Sedimentary Rocks, second edition. Prentice-Hall, Englewood Cliffs, NJ.

Brew G. & Barazangi M., 2001. Tectonic and geologic evolution of Syria. *GeoArabia* **6**: 573-616.

Chakraborty T. & Sensarma S., 2008. Shallow marine and coastal eolian quartz arenites in the Neoarchean–Palaeoproterozoic Karutola Formation, Dongargarh Volcano-sedimentary succession, central India. *Precambrian Research* **162**: 284-301.

Cocks L.R.M. & Torsvik T.H., 2002. Earth geography from 500 to 400 million years ago: a faunal and palaeomagnetic review. *Journal Geological Society of London* **159**: 631-644.

Cullers R.L., 2000. The geochemistry of shales, siltstones and sandstones of Pennsylvanian-Permian age, Colorado, USA: Implications for provenance and metamorphic studies. *Lithos* **51**: 181-203.

Cullers R.L. & Podkovyrov V.N., 2000. The source and origin of terrigenous sedimentary rocks in the Mesoproterozoic Ui group, southeastern Russia. *Precambrian Research* **117**: 157–183.

Cullers R.L., Barret T., Carlson R. & Robinson B., 1987. Rare earth element and mineralogical changes in Holocene soil and stream sediment: a case study in the Wet Mountains, Colorado, USA. *Chemical Geology* **63**: 275–295.

Dabbagh M.E. & Rogers J.J., 1983. Depositional environments and tectonic significance of the Wajid Sandstone of southern Saudi Arabia. *Journal of African Earth Sciences* **1**: 47-57.

Dickinson W.R, Beard L.S., Brakenridge G.R., Etjavec J.L., Ferguson RC., Inman K.F., Knepp R.A., Lindberg F.A. & Ryberg, P.T., 1983. Provenance of North American Phanerozoic sandstones in relation to tectonic setting. *Geological Society of American Bulletin* **94**: 222-235.

Dickinson W.R. & Suczek C.A., 1979. Plate tectonics and sandstone compositions. *American Association of Petroleum Geologist Bulletin* **63**: 2164–2182.

Dimitrivic M.D. 1973. Geology of Kerman region. Geological Survey of Iran. Institute for Geological and Mining Exploration and Investigation of Nuclear and Other Mineral Raw Materials, Reports, Yu/52, 334 pp. Belgrad.

Folk R.L., 1980. Petrology of Sedimentary Rocks. Hemphill Publishing Co. 182 p., Austin. Texas.

Gaeley W.K., 1977. Ophiolite obduction and geologic evolution of the Oman Mountains and adjacent areas. *Geological Society of America Bulletin* **88**: 1183-1191.

Ghavidel-Syooki M., 1994. Biostratigraphy and paleo-biogeography of some Paleozoic rocks at Zagros and Alborz Mountains, Iran. *Geology Survey of Iran Publication*, 168 p.

Gradstein M., Ogg J.G., Schmitz M.D. & Ogg G.M., 2012. The Geologic Time Scale 2012. Elsevier, 1176p.

Hairapetian V., Mohibullah M., Tilley L.J., Williams M., Miller C.G., Afzal J., Ghobadi Pour M. & Hejazi S.M., 2011. Early Silurian carbonate platform ostracods from Iran: a peri-Gondwanan fauna with strong Laurentian affinities. *Gondwana Research* **20**: 645-653.

Huckriede R,. Kursten M. & Venzlaff H., 1962. Zur Geologie des Gebietes zwischen Kerman und Sagand (Iran). *Beiheft zum geologischen Jahrbuch* **51**: 1-197.

Husseini M.I., 1991. Tectonic and depositional model of the Arabian and adjoining plates during the Silurian-Devonian. *American Association of Petroleum Geologists Bulletin* **75**: 108-120.

Ingersoll R.V., Bullard T.F., Ford R.L., Grimm J.P., Pickle J.D. & Sares S.W., 1984. The effect of grain size on detrital modes: A test of the Gazzi-Dickinson point-conting method. *Journal of Sedimentary Petrology* **54**: 103-116.

Jafarzadeh M. & Hosseini-Barzi M., 2008. Petrography and geochemistry of Ahwaz sandstone member of Asmari Formation, Zagros, Iran: implications on provenance and tectonic setting. *Revista Mexicana de Ciencias Geológicas* **25**: 247–260.

Khalifa M.A., Soliman H.E. & Wanas H.A., 2006. The Cambrian Araba Formation in northeastern Egypt: facies and depositional environments. *Journal of Asian Sciences* **27**: 873-884.

Khanehbad M., Moussavi-Harami R., Mahboubi A., Nadjafi M. & Mahmudy Gharaie M.H., 2012. Geochemistry of Carboniferous sandstones (Sardar Formation), East-Central Iran: Implication for provenance and tectonic setting. *Acta Geologica Sinica* **86**: 1200-1210.

Klein G.D., 1971. A sedimentary model for determining paleotidal range. *Geological Society American Bulletin* **82**: 2585-2592.

Klein G.D., 1998. Clastic tidalites - a partial retrospective view. *In*: Alexander C.R., Davis R.A.V. & Henry J. (*eds*.): Tidalites: Processes and Products. *SEPM Special Publication* **81**: pp. 5-14.

Laboun A.A., 2010. Paleozoic tectono-stratigraphic framework of the Arabian Peninsula. *Journal of King Saud University (Science)* **22**: 41-50.

Lasemi Y., 2001. Facies Analysis, Depositional Environments and Sequence Stratigraphy of the Upper Pre-Cambrian and Paleozoic Rocks of Iran. 180 p., *Geological Survey of Iran* (in Persian).

Longhitano S.G., Mellere D., Steel R.J. & Ainsworth R.B., 2012. Tidal depositional systems in the rock record: A review and new insights. *Sedimentary Geology* **279**: 2-22.

McBride E.F., 1985. Diagenetic processes that affect provenance determinations in sandstone. *In:* G.G. Zuffa (*ed*.): Provenance of Arenite: 95-113. The Netherlands, Reidel publication Co.

McLennan S.M., Hemming S., McDaniel D.K. & Hanson G.N., 1993. Geochemical approaches to sedimentation, provenance and tectonics. *In*: Johnsson M.J. & Basu A. (*eds*.), Processes Controlling the Composition of Clastic Sediments. *Geological Society of America Special Paper* **284**: 21–40.

Morton A.C., Davies J.R. & Waters R.A., 1992. Heavy minerals as a guide to turbidite provenance in the Lower Paleozoic Southern Welsh Basin: a pilot study. *Geological Magazine* **129**: 573–580.

Najafzadeh A., Jafarzadeh M. & Moussavi-Harami R., 2010. Provenance and tectonic setting of Upper Devonian sandstones from Ilanqareh Formation (NW Iran). *Revista Mexicana de Ciencias Geológicas* **27**: 545-561.

Roser B.P. & Korsch R.J., 1986. Determination of tectonic setting of sandstone - mudstone suites using SiO_2 content and K_2O/Na_2O ratio. *Journal of Geology* **94**: 635–650.

Roser B.P. & Korsch R.J., 1988. Provenance signatures of sandstone–mudstone suites determined using discriminant function analysis of major-element data. *Chemical Geology* **67**: 119–139.

Ruban D.A., Al-Husseini M. & Iwasaki Y., 2007. Review of Middle East Paleozoic plate tectonics. *GeoArabia* **12**: 35-56.

Ruttner A.W., Nabavi M.H. & Hajian, J., 1968. Geology of the Shirgesht area (Tabas area, east Iran). *Reports of the Geological Survey of Iran* **4**: 1-133.

Schwab F.L., 1975. Framework mineralogy and chemical composition of continental margin-type sandstone. *Geology* **3**:487–490.

Sengör A.M.C., 1987. Tectonics of the Tethysides: orogenic collage development in a collisional setting. *Annual Reviews of Earth Planet Science* **15**:213–244.

Sengör A.M.C., 1990. A new model for the late Palaeozoic-Mesozoic tectonic evolution of Iran and its implications for Oman. *In*: Robertson A.H.F., Searle M.P. & Ries A.C. (*eds*.): The Geology and Tectonics of the Oman Region. *Geological Society of London Special Publication* **49**: 797–831.

Sengör A.M.C., Altiner D., Cin A., Ustaomer T. & Hsu K.J., 1988. Origin and assembly of the Tethysides orogenic collage at the expense of Gondwana Land. *In*: Audley-Charles, M.G., Hallam, A. (*eds*.): Gondwana and Tethys. *Geological Society of London Special Publication* **37**: 119-181.

Sharland P.R., Archer R., Casey D.M., Davies R.B., Hall S.H., Hevard A.P., Horbury A.D. & Simmons M.D., 2001. Arabian Plate Sequence Stratigraphy. *GeoArabian Special Publication* **2**: 1-270.

Stampfli G., Marcoux J. & Baud A., 1991. Tethyan margins in space and time. *Palaeogeography, Palaeoclimatology, Paleecology* **87**: 373–409.

Stocklin J., 1968. Structural history and tectonics of Iran: A review. *American Association of Petroleum Geologists Bulletin* **52**: 1229-1258.

Stocklin J., 1974. Possible ancient continental margins in Iran. *In*: Burk C.A., and Drake C.L. (*eds*.): The Geology of Continental Margins: 873-887. *Springer-Verlag*.

Stocklin J., 1977. Structural correlation of the Alpine ranges between Devonian-Lower Carboniferous of Iran and Central Asia. *Memoires hors Serie de la Societe Geologique de France* **8**: 333-353.

Suttner L.J., Basu A. & Mack G.H., 1981. Climate and the origin of quartzarenites. *Journal of Sedimentary Petrology* **51**: 1235–1246.

Takin M., 1972. Iranian geology and continental drift in the Middle East. *Nature* **235**: 147-150.

Taylor S.R. & McLennan S.M., 1985. The Continental Crust: Its Composition and Evolution. 312 p., Blackwell Scientific Publications.

Torsvik T.H. & Cocks L.R.M., 2009. The Lower Palaeozoic palaeogeographical evolution of the northeastern and eastern peri-Gondwanan margin from Turkey to New Zealand. *In*: Basset M.G. (*eds*.): Early Palaeozoic Peri-Gondwana Terranes: New Insights from Tectonics and Biogeography. *Geological Society London Special Publications* **325**: 3–21.

Vahdati-Daneshmand F., Mosavvary F., Mahmudy Ghareei M.H. & Ghasemi A., 1995. Geological Map of Zarand, 1:100,000 Series. Sheet 7351, Geology Survey of Iran, Tehran.

Vail P.R., Mitchum R.M. & Thompson S., 1977. Seismic stratigraphy and global changes of sea level, part four: global cycles of relative changes of sea level. *American Association of Petroleum Geologists Memoir* **26**: 83-98.

Wanas H.A. & Abdel-Maguid N.M., 2006. Petrography and geochemistry of the Cambro-Ordovician Wajid Sandstone, southwest Saudi Arabia: implications for provenance and tectonic setting. *Journal of Asian Earth Sciences* **27**: 416–429.

Warren J.K., 2006. Evaporites: Sediments, Resources and Hydrocarbons. Springer-Verlag, Berlin & Heidelberg, 1035 p.

Wehrmann A., Yılmaz I., Yalçın M.N., Wilde V., Schindler E., Weddige K., Saydam Demirtas G., Özkan R., Nazik R.A., Nalcıo lu G., Kozlu H., Karslıo lu O., Jansen U. & Ertug K., 2010. Devonian shallow-water sequences from the North Gondwana coastal margin (Central and Eastern Taurides, Turkey): Sedimentology, facies and global events. *Gondwana Research* **17**: 546-560.

Weltje G.J. & von Eynatten H., 2004. Quantitative provenance analysis of sediment: review and outlook. *Sedimentary Geology* **171**: 1-11.

Wendt J., Kaufmann B., Belka Z., Farsan N. & Karimu-Bavandpur A., 2002. Devonian/Lower Carboniferous stratigraphy, facies patterns and palaeogeography of Iran. Part I. Southeastern Iran. *Acta Geologica Polonica* **52**: 129-168.

Wendt J., Kaufmann B., Belka Z., Farsan N. & Karimu-Bavandpur A., 2005. Devonian/Lower Carboniferous stratigraphy, facies patterns and palaeogeography of Iran Part II. Northern and central Iran. *Acta Geologica Polonica* **55**: 31-97.

Wilmsen M., Fürsich F.T., Seyed-Emami K.M., Majidifard R. & Taheri J., 2009. The Cimmerian Orogeny in northern Iran: tectono-stratigraphic evidence from the foreland. *Terra Nova* **21**: 211-218.

Wilmsen M., Fürsich F.T., Seyed-Emami K.M., Majidifard R. & Zamani-Pedram M., 2010. Facies analysis of a large-scale Jurassic shelf-lagoon: the Kamar-e-Mehdi Formation of east-central Iran. *Facies* **56**: 59-87.

Yan Z., Wang Z., Wang T., Yan Q., Xiao W. & Li J., 2006. Provenance and tectonic setting of clastic deposits in the Devonian Xicheng Basin, Qinling Orogen, Central China. *Journal of Sedimentary Research* **76**: 557-574.

Young S.W., 1976. Petrographic textures of detrital polycrystalline quartz as an aid to interpreting crystalline source rocks. *Journal of Sedimentary Petrology* **46**: 595–603.

Zaid S.M., 2012. Provenance, diagenesis, tectonic setting and geochemistry of Rudies sandstone (Lower Miocene), Warda Field, Gulf of Suez, Egypt. J*ournal of African Earth Sciences* **66-67**: 56-71.

Zand-Moghadam, H., Moussavi-Harami, R.,& Mahboubi, A., 2009. Tidal sediments analysis of Top Quartzite in East of Zarand in Kerman area. *Journal of Stratigraphy and Sedimentology* **37**: 1-18 [in Persian].

Zand-Moghadam H., Moussavi-Harami R. & Mahboubi, A., 2013a. Sequence stratigraphy of the Early-Middle Devonian succession (Padeha Formation) in Tabas Block, East-Central Iran: Implication for mixed tidal flat deposits. *Palaeoworld.* In print. [DOI: 10.1016/j.palwor.2013.06.002]

Zand-Moghadam H., Moussavi-Harami R. & Mahboubi, A., 2013b. Comparison of tidalites in siliciclastic, carbonate, and mixed siliciclastic-carbonate Systems: examples from Cambrian and Devonian deposits of East-Central Iran. *ISRN Geology*. In print. [DOI: 10.1155/2013/534761]

Zimmermann U. & Bahlburg H., 2003. Provenance analysis and tectonic setting of the Ordovician clastic deposits in the southern Puna Basin, NW Argentina. *Sedimentology* **50**: 1079-1104.